



OPEN Design of maglev train driven by reconnection electromagnetic launcher

Liang Dong[✉], Wenlong Jiang[✉], Xiaokun Xie & Hengyou Li

In order to continuously break through the speed of ground transportation and meet the social needs of more efficient transportation methods, the maglev train is a key research direction in the future. In this paper, the maglev train is taken as the research object. Based on the reconnection electromagnetic launch technology, a new concept of reconnection vehicle is proposed. The reconnection electromagnetic launcher is used as the power system of the maglev train to make the maglev train reach the expected speed smoothly. The feasibility of this situation is demonstrated from theory and simulation, and it is hoped that it can provide new ideas for the design of the power system of the future maglev train.

Transportation is one of the primary pillars of society, encompassing a range of individual systems and their interconnectedness aimed at meeting the demands for the movement of people and goods. Generally speaking, when ground transportation exceeds speeds of 400 km/h, aerodynamic drag under atmospheric pressure accounts for more than 80% of the total resistance, leading to uneconomical operational speeds and significant startup noise. These factors hinder the future development of high-speed ground transportation and make it challenging to achieve speeds exceeding 600 km/h. Therefore, pipeline transportation becomes an inevitable and necessary approach to achieve ultra-high-speed transportation^{1,2}.

In recent years, the introduction of concepts like Hyperloop has sparked interest in researching even faster transportation options, exceeding speeds of 600 km/h³. The traction system is one of the most crucial components of a high-speed maglev train system. A safe, stable, and reliable acceleration system is extremely important for maglev trains, especially for those exceeding speeds of 600 km/h. The traditional high-speed propulsion method for maglev trains uses linear induction motor (LIM) or linear synchronous motor (LSM) in Table 1. Their driving speed is dependent on the motor torque and power supply frequency. For the entire maglev system, the size of the air gap determines the maximum achievable operating speed. In Switzerland and Germany, for their maglev trains, they have chosen motor torque distributions of 231 mm and 258 mm to achieve an appropriate air gap. Due to limitations in the highest output frequency of existing high-power inverters, the motor stator's maximum frequency is approximately 300Hz. As a result, the highest theoretical driving speed for a linear synchronous motor is only about 550 km/h.

At the same time, maintaining the high-power conversion equipment for such a linear motor is installed on the train, leading to a reduced effective payload of the train. Additionally, this setup places higher demands on the overall size and seismic resistance of the train, making it more technologically challenging. In the long term, high-speed maglev transportation aspires to achieve speeds of up to 600 km/h, necessitating traction and propulsion systems with characteristics such as high efficiency, reliability, stable traction, and minimal lateral forces on the motor.

Therefore, developing an acceleration system that enables rapid acceleration and long-term high-speed operation is a crucial challenge for current ultra-high-speed maglev trains. Currently, in the military field, an advanced electromagnetic propulsion system has achieved propulsion speeds of over 1000 m/s, and electromagnetic catapult systems have been applied to accelerate the takeoff of carrier-based aircraft. Electromagnetic propulsion technology theoretically allows for high-speed propulsion of large mass objects and can utilize electromagnetic forces for acceleration and deceleration during the train's operation. Moreover, the drive components of the electromagnetic propulsion system can be independent of the train, reducing the overall weight of the maglev pipeline train, decreasing the difficulty of levitation, and effectively enhancing the energy efficiency and operational stability of the maglev pipeline train.

During its development, electromagnetic launch technology has evolved into three main research directions: rail-guided electromagnetic launch, coil-based electromagnetic launch, and repulsion-based electromagnetic launch^{6,7}. The first two approaches suffer from issues such as large currents that can cause erosion of existing rail

School of Electrical Engineering, Southwest Jiaotong University, Chengdu 610031, China. ✉email: ldong@home.swjtu.edu.cn; jwlong-edu@foxmail.com

Train type	Drive method	Velocity (km/h)
Japan HSST	LIM	110
American AMT	LIM	60
American GA	LSM	160
Germany TR	LSM	500
Japan MLU	LSM	581
American Maglev2000	LSM	500
Switzerland Swissmetro	LSM	500

Table 1. Comparison of maglev train drives in some countries^{4,5}.

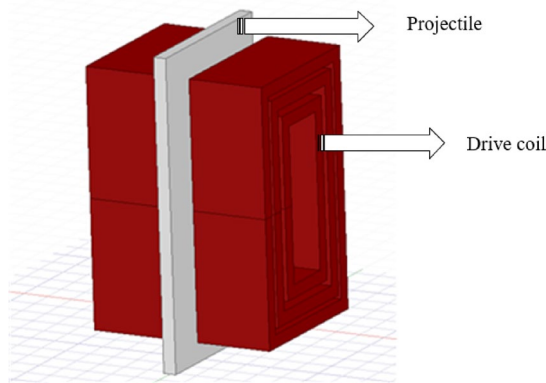


Fig. 1. Single-stage reconnection electromagnetic launch model. (Plotting with ANSYS Electronics Desktop 2019 R2. <https://www.ansys.com/zh-cn/products/electronics/ansys-maxwell>).

materials and radial electro-magnetic forces greater than axial forces. As the most recent of the three, repulsion-based electromagnetic launch technology can effectively avoid the problems faced by the previous two methods in principle. There is no contact between the armature and the driving coil, avoiding It solves the problems of ablation and friction loss during the launch process⁸⁻¹⁰. Moreover, the armature is mainly subjected to axial force rather than radial force during its launch. The reconnectable electromagnetic launcher was first proposed in 1986 and its feasibility has been proved¹¹.

Reconnection electromagnetic launching process

The plate-type reconnection electromagnetic launching system is the most basic among the reconnection electromagnetic launch systems. Many complex models, such as the multi-wing reconnections electromagnetic launching system and multi-pole moment reconnections electromagnetic launching system are constructed by combining multiple plate-type reconnection electromagnetic launching systems as shown in Fig. 1.

Figure 2 shows single-stage reconnection electromagnetic launch model driving circuit. The driving circuit of the reconnection type electromagnetic launcher is composed of pulse capacitor, diode, controlled switch, equivalent device resistor, and equivalent inductor. When the switch is closed, the pulse capacitor begins to discharge. When the capacitor is fully discharged, the switch is disconnected, and the current will flow through the freewheeling diode to the drive coil until the launch process is completed.

When the capacitor discharges completely, the diode begins to conduct, and the circuit equation can be expressed as follows:

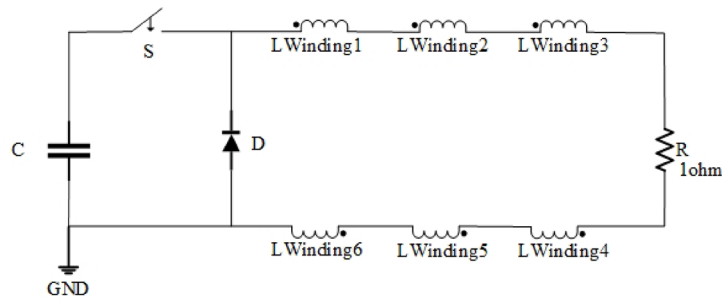
$$\frac{d(Li)}{dt} + Ri = 0 \quad (1)$$

Solve the Eq. (1)

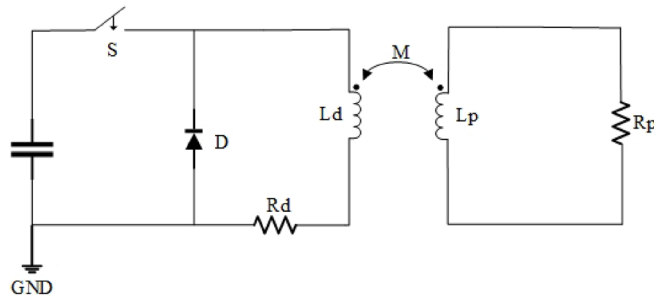
$$i = \frac{I_0 L_0}{L} \exp\left(-\int_0^t \frac{R}{L} dt\right) \quad (2)$$

In the equation, L represents the equivalent inductance of the RLC circuit, R is the equivalent resistance, I_0 is the initial current flowing through L , $I_0 = i(0)$, L_0 is the equivalent initial inductance, $L_0 = L(0)$.

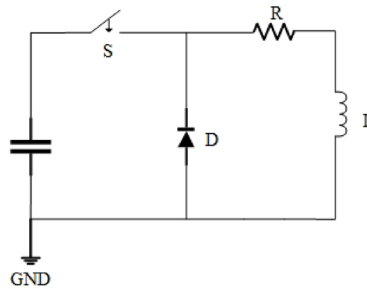
Electromagnetic energy stored in an inductor can be calculated using the following formula:



(a) Simulation circuit diagram



(b) Equivalent circuit



(c) RLC circuit

Fig. 2. Single-stage reconnection electromagnetic launch model driving circuit.

$$E_m = \frac{Li^2}{2} = \frac{L \left\{ \frac{I_0^2 L_0^2}{L^2} \left[\exp \left(- \int_0^t \frac{R}{L} dt \right) \right]^2 \right\}}{2} \tag{3}$$

Simultaneous (2) and (3), get

$$E_m = \frac{E_{m0} L_0}{L} \exp \left(-2 \int_0^t \frac{R}{L} dt \right) \tag{4}$$

The reconnection electromagnetic launch system typically uses pulse capacitors for energy supply. A portion of the electrical energy is converted into mechanical energy, ultimately transforming into kinetic energy of the armature, leading to an increase in the armature's velocity. Another portion of the electrical energy is converted into magnetic energy, increasing the magnetic field around the driving coil.

At any time t , the total energy $W(t)$ of the system can be expressed as:

$$W(t) = \frac{Q^2(t)}{2C} + \frac{1}{2}i^2(t)L[x(t)] + \frac{1}{2}mv^2(t) \quad (5)$$

In formula (5), $Q(t)$ is the charge of the capacitor, which is a function of time t ; C is the capacitance value; $i(t)$ is the current of the driving coil, which is a function of time t ; $L[x(t)]$ is the equivalent inductance in the electro-magnetic propulsion device, including the self-inductance of the coil and the armature, the mutual inductance between the two driving coils, and the mutual inductance between the coil and the armature, $L[x(t)]$ is a function of the relative position of the coil and the armature; m is the mass of the armature, and $v(t)$ is the speed of the armature, which is a function of time t .

At time t , the total energy of the system $W(t + \Delta t)$ can be expressed as:

$$W(t + \Delta t) = \frac{Q^2(t + \Delta t)}{2C} + \frac{1}{2}i^2(t + \Delta t)L[x(t + \Delta t)] + \frac{1}{2}mv^2(t + \Delta t) \quad (6)$$

According to the law of conservation of energy, considering only the ohmic loss of the entire device between t and $(t + \Delta t)$, we can obtain:

$$-Ri^2(t) = \lim_{\Delta t \rightarrow 0} \frac{W(t + \Delta t) - W(t)}{\Delta t} = \frac{Q(t)}{C} \frac{dQ(t)}{dt} + \frac{1}{2} \frac{d[i^2(t)L[x(t)]]}{dt} + mv(t) \frac{dv(t)}{dt} \quad (7)$$

where R is the equivalent resistance in the reconnection type electromagnetic propulsion device.

From Fig. 2, we can see that the loop voltage after the capacitor is discharged can be expressed as:

$$-Ri(t) = -\frac{Q(t)}{C} + \frac{d[L[x(t)]i(t)]}{dt} \quad (8)$$

where $\frac{d[L[x(t)]i(t)]}{dt}$ can be decomposed into

$$\frac{d[L[x(t)]i(t)]}{dt} = \frac{i(t)dL[x(t)]}{dt} + \frac{L[x(t)]di(t)}{dt} \quad (9)$$

Multiply both sides of formula (8) by $i(t)$:

$$-Ri^2(t) = -\frac{Q(t)}{C}i(t) + \frac{d[L[x(t)]]}{dt}i^2(t) + L[x(t)]i(t)\frac{d[i(t)]}{dt} \quad (10)$$

From formulas (7), (8) and (10), it can be deduced that:

$$mv(t)\frac{dv(t)}{dt} = \frac{1}{2} \frac{d[L[x(t)]]}{dt}i^2(t) \quad (11)$$

Formula (11) can finally be expressed as:

$$F(t) = m\frac{dv(t)}{dt} = \frac{1}{2} \frac{d[L[x(t)]]}{dx}i^2(t) \quad (12)$$

$\frac{d[L[x(t)]]}{dx}$ is the inductance gradient. Formula (12) establishes a relationship between electrical quantities and force quantities, which can characterize key parameters of electromagnetic launch.

Simulation

By using finite element simulation tools, a single-stage reconnection electromagnetic launching device was established, utilizing a 15 kV 400 μ F capacitor as the pulse power source in vacuum. In order to enhance the magnetic field of the driving coil, a three-layer coil is used as the driving coil. Setting the armature to a certain initial position will make the induced current on the trailing edge of the armature more concentrated. The Fig. 3 shows the magnetic field distribution of the winding when the current is turned on, and the Fig. 4 illustrates the induced current in the aluminum flyer due to external magnetic field variations. The presence of this induced current causes the aluminum flyer to experience Ampere forces in the applied magnetic field, resulting in high velocity and acceleration. As the induced current gradually decreases, the velocity of the aluminum flyer stabilizes. From the graph, it can be observed that within 0.5 ms, the device accelerates the armature to 40 m/s.

The reconnection electromagnetic launch device has a strong acceleration capability, and the device does not have electrical contact, and will not generate a large amount of frictional heat loss due to mechanical movement, which can reduce mechanical fatigue and material strength requirements. Fig. 5 shows the velocity of armature. Theoretically, the upper limit of the speed of the device can fully reach the ideal running speed of a maglev train of 600 km/h.

Reconnection vehicle

Based on the high acceleration capability of the reconnection electromagnetic launcher, a maglev train using the reconnection electromagnetic launcher as the power system is proposed, as shown in the Fig. 6 (Table 2).

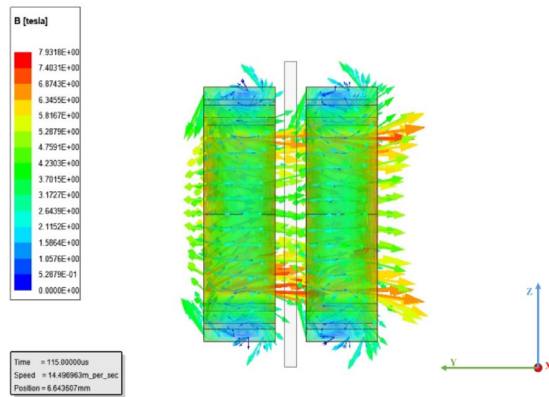


Fig. 3. Magnetic field distribution.

Figure 7 shows the electromagnetic field distribution of the reconstructor at a certain moment. The driving coil generates a magnetic field in the negative direction of the Y axis. At this time, the aluminum armature generates a clockwise current in the XOZ plane. However, due to the large current at the rear edge of the armature, the armature is subjected to a driving force in the positive direction of the X axis under the action of the magnetic field in the negative direction of the Y axis.

To apply single-stage reconnection electromagnetic launching device to the train's propulsion system, an energy recovery system should also be incorporated. This is because during the operation, a significant amount of energy is stored in the form of magnetic energy in the windings. When the armature detaches from the acceleration winding, this portion of energy can be recovered through an external energy recovery device. This will greatly enhance the overall system's energy efficiency, as shown in the Fig. 8.

The introduction of an energy recovery system is not only beneficial for energy conservation but also reduces reliance on external energy sources, leading to lower train operation costs. Consequently, the entire train system becomes more environmentally friendly and economically efficient¹².

The high acceleration demonstrated by single-stage reconnection electromagnetic launching device, as mentioned earlier, is too high for a passenger maglev train. It can be regulated by adjusting the pulse magnitude and duration of the energy supply device, as well as controlling the inductance of the windings and the induced current in the armature.

When the current in the windings is as shown in Fig. 9, the change in the train's velocity graph indicates a relatively smooth acceleration, approximately 20 m/s^2 . Figure 10 shows the speed variation of the reconnection vehicle. The fluctuation trend of the propulsive force also aligns with the change in the winding current. If the current variation in the winding coil can be maintained consistent with the trend in the first 2 ms as shown in Fig. 9, the maglev train's velocity will reach around 100 km/h at about 1.4 seconds and achieve its operational speed of 600 km/h within 10 seconds. This level of acceleration capability is challenging for conventional linear motors to achieve currently.

Results

Considering the growing demand for high-speed transportation in the current social production and life, and the continuous exploration of the acceleration device of the future maglev train, this paper proposes a new power plant design for the maglev train based on the reconnection electromagnetic launch device. By expounding the acceleration principle of reconnection electromagnetic propulsion, it can be found that compared with linear motors and other power devices, this type of propulsion has basically no mechanical friction, less device loss, and stronger acceleration capabilities. As a possible new technology, the reconnection vehicle requires further optimization, but if this technology is applied to the driving system of the vacuum maglev train, the upper limit of the speed of the train will be higher. This paper can provide a new thinking reference for the development of the power plant of the maglev train in the future.

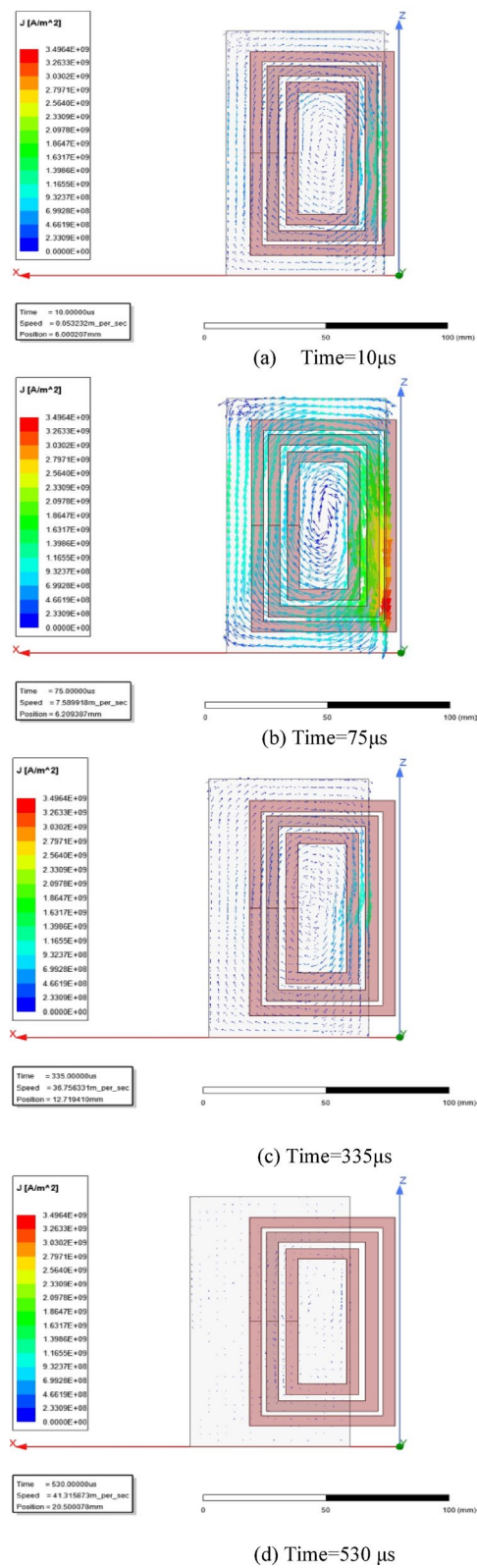


Fig. 4. Vortex and position distribution of armature.

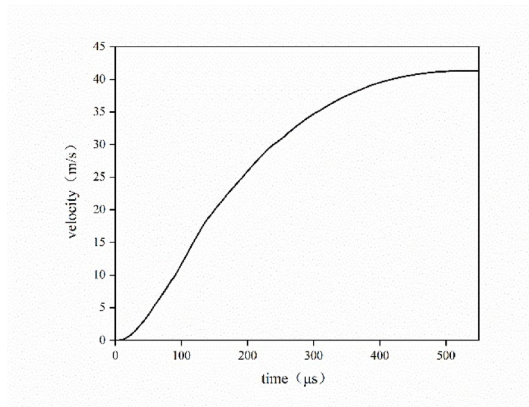
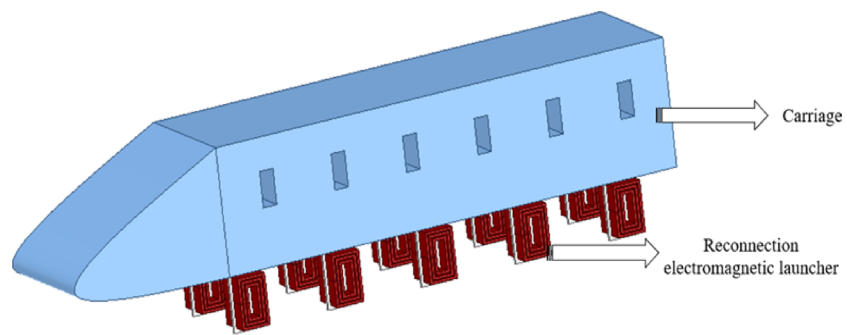
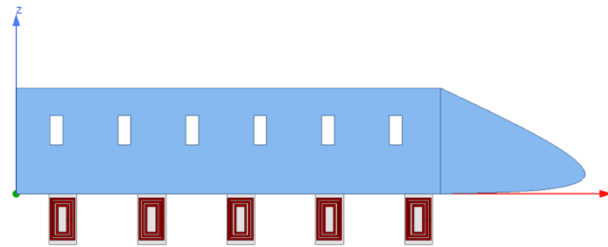


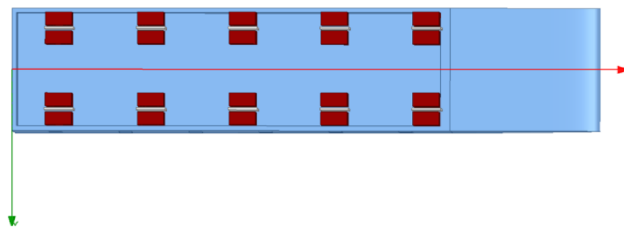
Fig. 5. Velocity of armature.



(a) Composition of the reconnection vehicle



(b) Side view of the reconnection vehicle



(c) Bottom view of the reconnection vehicle

Fig. 6. Reconnection vehicle.

Components	Parameter	Value
Coil	Outer Rectangle/mm	60*100 46*86 30*70
	Inner Rectangle/mm	50*90 36*76 20*60
	Thickness/mm	30
	Number of Coil Turns	15
	Material	Copper
	Number	20
	Wing Length/mm	66
Drive plate	Thickness /mm	5
	Highness/mm	120
	Material	Aluminum
	Number	10
	Length/mm	1000
Carriage	Width /mm	280
	Height/mm	286
	Material	Aluminum
	Mass/kg	108

Table 2. Launch model parameters.

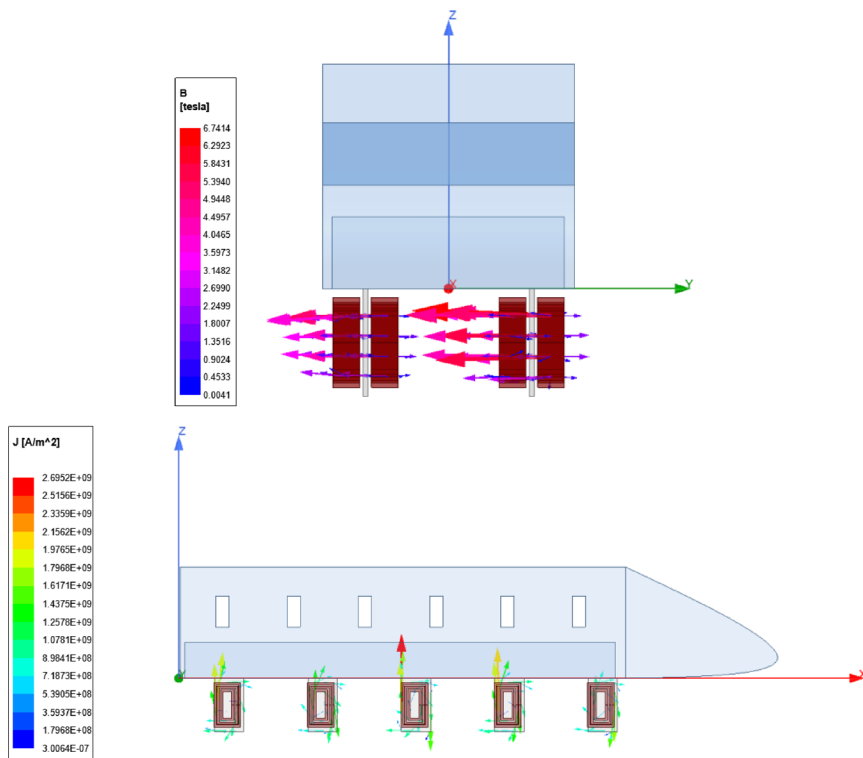


Fig. 7. Electromagnetic distribution of the reconnection vehicle. (Plotting with ANSYS Electronics Desktop 2019 R2. <https://www.ansys.com/zh-cn/products/electronics/ansys-maxwell>).

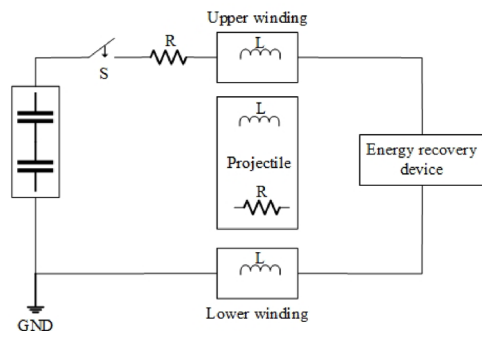


Fig. 8. Schematic diagram of the drive system.

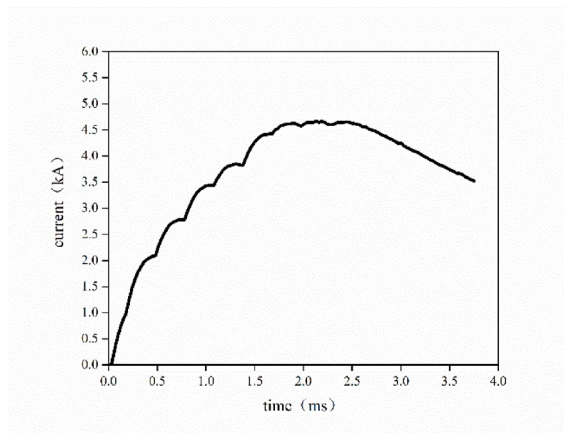


Fig. 9. Winding current.

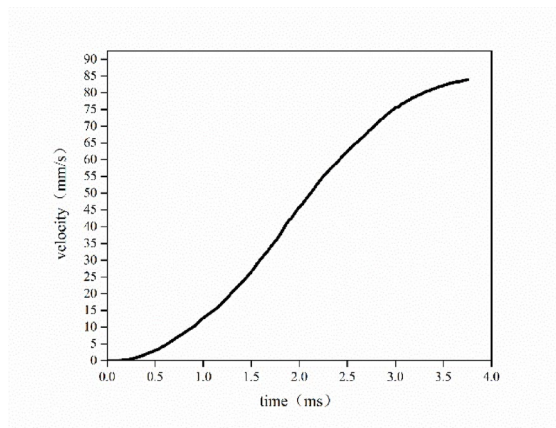


Fig. 10. Velocity of reconnection vehicle.

Data availability

All data generated or analysed during this study are included in this published article.

Received: 11 April 2025; Accepted: 5 June 2025

Published online: 02 July 2025

References

1. Gkoumas, K. & Christou, M. A Triple-helix approach for the assessment of hyperloop potential in Europe. *Sustainability* **12**(19), 7868 (2020).

2. Thornton, R. D. Efficient and affordable maglev opportunities in the United States. *Proc. IEEE* **97**(11), 1901–1921 (2009).
3. Lim, J. et al. Equivalent inductance model for the design analysis of electrodynamic suspension coils for hyperloop. *Sci. Rep.* **11**(1), 23499 (2021).
4. Lv, G. Review of the application and key technology in the linear motor for the rail transit. *Proc. CSEE*. **40**(17), 5665–5675 (2020).
5. Lu, Q., Li, Y., Ye, Y. & Zhu, Z. Q. Investigation of forces in linear induction motor under different slip frequency for low-speed maglev application. *IEEE Trans. Energy Convers.* **28**(1), 145–153 (2013).
6. Qiu, J., Song, S., Liao, M., Duan, X. & Zhou, X. Armature structure research of an electromagnetic reconnection launcher. *IEEE Trans. Plasma Sci.* **50**(8), 2403–2411 (2022).
7. Kaye, R. J. et al. Design and performance of a multi-stage cylindrical reconnection launcher. *IEEE Trans. Magn.* **27**(1), 596–600 (1991).
8. Cowan, M., Cnare, E., Duggin, B., Kaye, R. & Tucker, T. The reconnection gun. *IEEE Trans. Magn.* **22**(6), 1429–1434 (1986).
9. Zhang, T., Guo, W., Su, Z. & Cao, B. Investigation of magnetic field arrangement on launching performance of multistage synchronous induction coilgun. *IEEE Trans. Plasma Sci.* **45**(7), 1436–1442 (2017).
10. Cowan, M. et al. Exploratory development of the reconnection launcher 1986–90. *IEEE Trans. Magn.* **27**(1), 563–567 (1991).
11. Widner, M. M. WARP-10: A numerical simulation model for the cylindrical reconnection launcher. *IEEE Trans. Magn.* **27**(1), 634–638 (1991).
12. Fan, G. et al. Research on energy conversion efficiency of the reconfigurable reconnection electromagnetic launcher. *Energy* **215**, 119088 (2021).

Acknowledgements

This work was supported by National Natural Science Foundation of China under Grant 52372399, Sichuan Provincial Natural Science Foundation of China Project under Grant 2023NSFSC0397 and Foundation of Key Laboratory of Magnetic Suspension Technology and Maglev Vehicle, Ministry of Education.

Author contributions

D.L. conceived and mainly wrote this article. W.J. and X.X. conducted the simulations, H.L. analysed the results. All authors reviewed the manuscript.

Declarations

Competing interests

The authors declare no competing interests.

Additional information

Correspondence and requests for materials should be addressed to L.D. or W.J.

Reprints and permissions information is available at www.nature.com/reprints.

Publisher's note Springer Nature remains neutral with regard to jurisdictional claims in published maps and institutional affiliations.

Open Access This article is licensed under a Creative Commons Attribution-NonCommercial-NoDerivatives 4.0 International License, which permits any non-commercial use, sharing, distribution and reproduction in any medium or format, as long as you give appropriate credit to the original author(s) and the source, provide a link to the Creative Commons licence, and indicate if you modified the licensed material. You do not have permission under this licence to share adapted material derived from this article or parts of it. The images or other third party material in this article are included in the article's Creative Commons licence, unless indicated otherwise in a credit line to the material. If material is not included in the article's Creative Commons licence and your intended use is not permitted by statutory regulation or exceeds the permitted use, you will need to obtain permission directly from the copyright holder. To view a copy of this licence, visit <http://creativecommons.org/licenses/by-nc-nd/4.0/>.

© The Author(s) 2025